Parallel activation of Ca2+-induced survival and death pathways in cardiomyocytes by sorbitol-induced hyperosmotic stress

Article *in* Apoptosis · May 2010

DOI: 10.1007/s10495-010-0505-9 · Source: PubMed

17 authors, including:

Mario Chiong
University of Chile
153 PUBLICATIONS **3,597** CITATIONS

SEE PROFILE

Valentina Parra
University of Chile
53 PUBLICATIONS **1,776** CITATIONS

SEE PROFILE

Veronica Eisner
Pontificia Universidad Católica de Chile
45 PUBLICATIONS **681** CITATIONS

SEE PROFILE

Apoptosis (2010) 15:887–903
DOI 10.1007/s10495-010-0505-9

ORIGINAL PAPER

Parallel activation of Ca^{2+}-induced survival and death pathways in cardiomyocytes by sorbitol-induced hyperosmotic stress

M. Chiong · V. Parra · V. Eisner · C. Ibarra · C. Maldonado · A. Criollo · R. Bravo · C. Quiroga · A. Contreras · J. M. Vicencio · P. Cea · J. L. Bucarey · J. Molgó · E. Jaimovich · C. Hidalgo · G. Kroemer · S. Lavandero

Published online: 8 May 2010

Abstract Hyperosmotic stress promotes rapid and pronounced apoptosis in cultured cardiomyocytes. Here, we investigated if Ca^{2+} signals contribute to this response. Exposure of cardiomyocytes to sorbitol [600 mosmol (kg water)$^{-1}$] elicited large and oscillatory intracellular Ca^{2+} concentration increases. These Ca^{2+} signals were inhibited by nifedipine, Cd^{2+}, U73122, xestospongin C and ryanodine, suggesting contributions from both Ca^{2+} influx through voltage dependent L-type Ca^{2+} channels plus Ca^{2+} release from intracellular stores mediated by IP_3 receptors and ryanodine receptors. Hyperosmotic stress also increased mitochondrial Ca^{2+} levels, promoted mitochondrial depolarization, reduced intracellular ATP content, and activated the transcriptional factor cyclic AMP responsive element binding protein (CREB), determined by increased CREB phosphorylation and electrophoretic mobility shift assays. Incubation with 1 mM EGTA to decrease extracellular [Ca^{2+}] prevented cardiomyocyte apoptosis induced by hyperosmotic stress, while overexpression of an adenoviral dominant negative form of CREB abolished the cardioprotection provided by 1 mM EGTA. These results suggest that hyperosmotic stress induced by sorbitol, by increasing Ca^{2+} influx and raising intracellular Ca^{2+} concentration, activates Ca^{2+} release from stores and causes cell death through mitochondrial function collapse. In addition, the present results suggest that the Ca^{2+} increase induced by hyperosmotic stress promotes cell survival by recruiting CREB-mediated signaling. Thus, the fate of cardiomyocytes under hyperosmotic stress will depend on the balance between Ca^{2+}-induced survival and death pathways.

Keywords Cardiomyocyte · Hyperosmotic stress · Sorbitol · Calcium · Metabolic collapse · CREB

M. Chiong, V. Parra and V. Eisner contributed equally to this work.

Electronic supplementary material The online version of this article (doi:10.1007/s10495-010-0505-9) contains supplementary material, which is available to authorized users.

M. Chiong · V. Parra · V. Eisner · C. Ibarra · C. Maldonado · A. Criollo · R. Bravo · C. Quiroga · A. Contreras · J. M. Vicencio · P. Cea · J. L. Bucarey · E. Jaimovich · C. Hidalgo · S. Lavandero
Centro FONDAP Estudios Moleculares de la Célula, Universidad de Chile, Santiago, Chile

S. Lavandero (✉)
Departamento de Bioquímica y Biología Molecular, Facultad de Ciencias Químicas y Farmacéuticas, Universidad de Chile, Olivos 1007, 8380492 Santiago, Chile
e-mail: slavander@uchile.cl

S. Lavandero
Division of Cardiology, Department of Internal Medicine, University of Texas Southwestern Medical Center, Dallas, TX 75235, USA

E. Jaimovich · C. Hidalgo · S. Lavandero
Instituto de Ciencias Biomédicas, Facultad de Medicina, Universidad de Chile, 8380492 Santiago, Chile

J. Molgó
Centre National de la Recherche Scientifique, Institut de Neurobiologie Alfred Fessard, FRC2118, UPR 9040, 91198 Gif-sur-Yvette, France

G. Kroemer
Institut Gustave Roussy, 39 rue Camille Desmoulins, 94805 Villejuif, France

Abbreviations

AdLacZ	Adenovirus β-galactosidase
Ad dnCREB	Adenovirus dominant negative CREB
AIF	Apoptosis inducing factor
$[Ca^{2+}]i$	Intracellular calcium concentration
CICR	Ca^{2+}-induced Ca^{2+} release
CaMK	Calmodulin kinase
CREB	Cyclic AMP responsive element binding protein
CsA	Cyclosporin A
ERK	Extracellular signal-regulated kinase
fluo3-AM	Fluo3 acetoximethylester
IP3	Inositol-1,4,5-trisphosphate
IP3R	IP3 receptor
LY	LY294002
MAPK	Mitogen activated protein kinase
MOI	Multiplicity of infection
p38	p38-Mitogen activated protein kinase
PD	PD98059
PLC	Phospholipase C
RuRed	Ruthenium red
SB	SB203580
SERCA	Sarco/endoplasmic reticulum Ca^{2+}-ATPase
TMRM	Tetramethylrhodamine methyl ester

Introduction

Cardiovascular diseases are the leading cause of death in developed countries [1]. Loss of cardiomyocytes due to cell death is an important factor in the development of cardiac morbidity. Thus, cardiomyocyte survival in response to stress is critical for normal heart function [2, 3]. Cardiac myocyte apoptosis can be induced by various stimuli, including osmotic stress [4]. Osmotic changes can occur in pathological states such as ischemia, septic shock and diabetic coma. In the heart, osmotic stress can develop during a period of myocardial ischemia [5].

Hyperosmotic stress stimulates rapid and pronounced apoptosis in cultured cardiomyocytes [4]. Hypertonic stress may also activate survival-signaling cascades, so that the balance between death and survival pathways will determine the fate of the cell. Cardiomyocytes may survive hypertonic stress through diverse compensatory mechanisms, including accumulation of organic osmolytes and induction of heat shock proteins [6–8]. Although induction of aldose reductase has been associated with compensatory mechanisms against hyperosmotic stress [9], we have shown previously that aldose reductase activation is required for sorbitol-induced cardiomyocyte apoptosis [10].

The involvement of elevated Ca^{2+} signals in cell death has been widely described [11, 12], and Ca^{2+} overload has been suggested as the final common pathway of all types of cell death [12]. Several studies have shown that cytoplasmic $[Ca^{2+}]$ increases at both early and late stages of the apoptotic process [13–17]. Both Ca^{2+} release from the endoplasmic reticulum and capacitative Ca^{2+} influx through Ca^{2+} release-activated Ca^{2+} channels may be apoptogenic [18–20]. Yet, Ca^{2+} is also associated with survival signaling. The Ca^{2+}-activated transcription factor cAMP responsive element binding protein (CREB) has been widely described in several cell types as an anti-apoptotic transcription factor [21, 22]. CREB activity is regulated by the phosphorylation of several serine residues, most notably Ser-133. Ca^{2+}-dependent activation of multiple protein kinases, including calmodulin kinase (CaMK), mitogen activated protein kinase (MAPK) and protein kinase A lead to CREB activation through Ser-133 phosphorylation [23, 24].

There has been much interest in the mechanisms connecting alterations in Ca^{2+} signaling with the execution of apoptosis, as well as on the effects of Ca^{2+} on inducing cell survival or necrosis. Accordingly, the aim of this work was to investigate if Ca^{2+} signals contribute to the response of cardiomyocytes to sorbitol-induced hyperosmotic stress.

Materials and methods

Materials

Thapsigargin, xestospongin C, LY294002 (LY), PD98059 (PD) and SB203580 (SB) were from Calbiochem. U-73122, caffeine, ryanodine, nifedipine, sorbitol and other biochemical reagents were from Sigma.

Culture of cardiomyocytes

Rats were bred in the Animal Breeding Facility at the Faculty of Chemical and Pharmaceutical Sciences, Universidad de Chile (Santiago, Chile). This investigation conforms to the "Guide for the care and use of laboratory animals" published by the U.S. National Institutes of Health (NIH publication No. 85-23, revised 1985). Cardiomyocytes were prepared from hearts of 1–3-day-old Sprague–Dawley rats as described previously [25]. Briefly, ventricles were trisected, pooled and cardiomyocytes were dissociated in a solution containing collagenase and pancreatin. After enzymatic dissociation, cells were selectively enriched in cardiac myocytes by pre-plating in DMEM:M199 (4:1) containing 10% (v/v) horse serum, 5% (v/v) heated-inactivated fetal calf serum, penicillin and streptomycin (100 units/ml). Cardiomyocytes were plated at a final density of 1–8 $\times$ 10^3/mm^2 on gelatin-coated Petri dishes. For detection of Ca^{2+} signals and immunocytochemistry, cells

were plated at a final density of $1.0 \times 10^3/mm^2$ on gelatin-precoated coverslips. Cardiomyocytes were plated for 16–18 h and then serum was withdrawn for 24 h before exposure to sorbitol [600 mosmol $(kg\ water)^{-1}$ or other concentrations as indicated] dissolved in serum-free DME/M199. Cell cultures contained at least 95% cardiomyocytes.

Measurement of intracellular and mitochondrial Ca^{2+} levels

Cellular Ca^{2+} images were obtained from cardiomyocytes pre-loaded with fluo3 acetoximethylester (fluo3-AM, Molecular Probes) using either an inverted confocal microscope (Carl Zeiss Axiovert 135 M LSM Microsystems) or a fluorescence microscope (Olympus Diaphot-TMD, Nikon Corporation) equipped with a cooled CCD camera and an image acquisition system (Spectra Source MCD 600), as previously described [26]. Mitochondrial and cytoplasmic Ca^{2+} levels were simultaneously measured in cultured cardiomyocytes preloaded with fluo3-AM or rhod2-AM using an inverted confocal microscope (Carl Zeiss LSM-5, Pascal 5 Axiovert 200 microscope).

Cell-containing coverslips were mounted in a 1-ml capacity chamber and placed in the microscope for fluorescence or confocal measurements after excitation with a laser lamp or laser line, respectively (excitation 488-nm; emission 526 nm for fluo3-AM and excitation 543; emission 580 nm for rhod2-AM). Sorbitol was either added directly (2× solution) or the solution was rapidly exchanged in the camera (1 s). Fluorescent images were collected every 0.4–2.0 s for fast signals and analyzed frame by frame with the Image J software (NIH, Bethesda, MD). For intracellular Ca^{2+} measurements, a manual contour of the whole cell was generated while for mitochondrial Ca^{2+} determinations, an optical region of interest (ROI) on perinuclear mitochondria was analyzed. To quantify fluorescence, the summed pixel intensity was calculated from the section delimited by the whole cell contour or the mitochondrial ROI. Intracellular Ca^{2+} levels are expressed as relative fluorescence, $\Delta F/F_0$, where ΔF represents the difference between the experimental value F and the basal fluorescence value F_0. Within the range defined for each probe, the fluorescence intensity increases proportionally with intracellular Ca^{2+} concentration [26]. Digital image processing was performed as previously described [26]. In other additional experiments, cytoplasmic Ca^{2+} levels were also measured with the ratiometric Ca^{2+} probe Fura2. To this aim, cardiomyocytes were loaded with fura2 AM (5 μM) for 30 min. Cells were placed on a 0.5 ml chamber in an inverted microscope (Olympus) equipped with epi-fluorescence illumination provided by a Xenon lamp. The dye within a single cell was excited at 340 and 380 nm using filters displayed in a filter wheel, and the intensity of the emitted fluorescence was monitored at 510 nm with a photomultiplier tube associated to a Fluorescence System Interface and Acquisition System Software (Ion Optix Corp., Milton, MA). When using Fura2, values were expressed as F340/F380 ratios.

Experimental determinations were carried out in cardiomyocytes bathed with Ca^{2+}-containing Krebs buffer (140 mM NaCl, 5 mM KCl, 1 mM $CaCl_2$, 1 mM $MgCl_2$, 10 mM HEPES, 1 mg/ml glucose); Ca^{2+}-containing Krebs buffer supplemented with 1 mM EGTA Krebs buffer (1.8 mM $CaCl_2$, 0.2 mM $MgCl_2$, 1 mM EGTA), or Ca^{2+}-free Krebs buffer (without $CaCl_2$, plus 2 mM $MgCl_2$ and 1 mM EGTA). In the experiments where inhibitors were used, cardiomyocytes were incubated with both, the dye and the inhibitor during a period of 30 min before the Ca^{2+} measurements.

Measurement of mitochondrial depolarization

Cardiomyocytes were pre-loaded with 100 nM TMRM (Molecular Probes) for 17 min a 37°C and images were acquired with an inverted confocal microscope (excitation 543 nm; emission 500–600 nm). Measurements are expressed as percentage of fluorescence intensity relative to basal fluorescence. Maximum mitochondrial depolarization was obtained using the protonophore CCCP (carbonyl cyanide 3-chlorophenylhydrazone, 10 μM).

Western blotting

Protein extracts were prepared from cardiomyocytes as described [10]. Samples containing equal amounts of protein were resolved by SDS–PAGE, transferred to nitrocellulose membranes (Bio-Rad Laboratories) and probed with specific antibodies against p-CREB^{133} Ser133, CREB, caspase 9 or caspase 3 (Cell Signaling). After an additional incubation period with appropriate secondary HRP-coupled antibodies (Calbiochem), blots were developed by chemiluminescence using the ECL system (Perkin Elmer).

Electrophoretic Mobility Shift Assay (EMSA) and supershift assays

CRE oligonucleotide 5′-GAGATTGCCTGACGTCAGAGAGCTA G-3′ was end-labeled with T4 kinase and [γ^{32}P]-ATP (75 μCi, Amersham). The ^{32}P-oligonucleotides (30,000 cpm) were incubated for 20 min at 4°C in a 25 μl reaction mixture containing 2 μg of nuclear proteins, 10 mM Tris–HCl (pH 7.5), 500 ng poly (dG-dC), 5 mM $MgCl_2$, 1 mM EDTA, 12.5% (v/v) glycerol, 1 mM DTT, 0.1% (v/v) Triton X-100 and analyzed on 6% polyacrylamide gels in 0.5% Tris–borate–EDTA buffer. Supershift assays were performed incubating nuclear extracts (5 μg)

with 2 μg of anti CREB antibody (Cell Signaling) for 2 h at room temperature. As controls, 100-fold excess of non-radioactive CRE and 1,000-fold excess of mutated oligonucleotides (5′-AGAGATTGCCTGTGGTCAGAGAGCT AG-3′) were used.

Immunocytochemistry

Cardiomyocytes grown on coverslips, fixed for 10 min with PBS containing 4% paraformaldehyde, were permeabilized with 0.3% Triton X-100 for 10 min. Nonspecific sites were blocked for 1 h with 5% BSA in PBS. Cells were then incubated with AIF (Chemicon) or cytochrome c antibodies (BD Pharmingen) at 1:100 or 1:400 dilutions, respectively. Cardiomyocytes were washed with PBS and incubated with anti-rabbit or anti-mouse IgG-Alexa488 secondary antibody, respectively. Nuclei were stained with 5 μg/ml propidium iodide (PI). Coverslips were mounted in DakoCytomation fluorescent mounting medium (DakoCytomation). The resulting fluorescence was evaluated in a scanning confocal microscope (Carl Zeiss Axiovert 135, LSM Microsystems).

Apoptosis and ATP content determinations

The number of viable cells was determined by the trypan blue exclusion method as described [27]. DNA fragmentation was determined as described previously [10]. Caspase 9 activity was measured using the colorimetric caspase-3 substrate Ac-LEHD-pNA (Calbiochem) [28]. ATP content was determined using the luciferin/luciferase assay as described [29].

Recombinant adenoviruses

Dr. Charles Vinson (NIH, Bethesda, USA) provided Ad dnCREB, which over expresses a dominant negative form of CREB (Ser133/Ala) [30]. Cardiomyocytes were transduced with Ad dnCREB or β-galactosidase (Ad LacZ) at a multiplicity of infection (MOI) of 300 and cultivated 24 h prior to sorbitol stimulation [26].

Expression of results and statistical analysis

Data shown correspond to the mean ± SEM of the number of independent experiment indicated (n); alternatively, representative experiments, performed on at least three separate occasions with similar outcome, are shown. Data were analyzed by ANOVA and comparisons between groups were performed using a protected Tukey's test. A value of $P < 0.05$ was set as the limit of statistical significance.

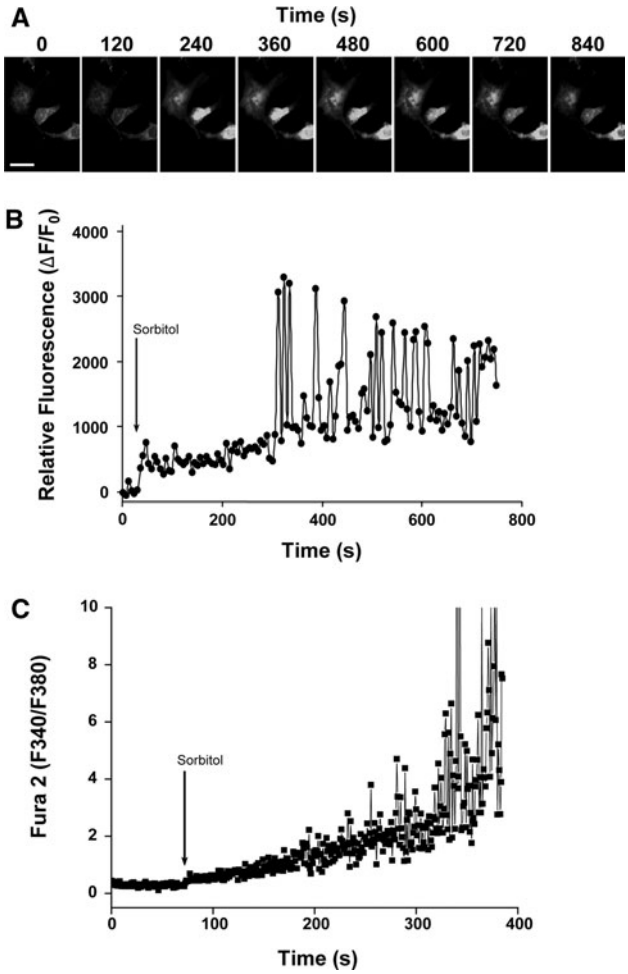

Fig. 1 Hyperosmotic stress increases intracellular Ca^{2+} concentration in cultured cardiomyocytes. Cells preloaded with fluo3-AM (**a**, **b**) or fura2-AM (**c**) were perfused at the time indicated with an *arrow* with Ca^{2+}-containing Krebs buffer supplemented with sorbitol (Sor) [600 mosmol (kg water)$^{-1}$]. Using a fluorescence microscope equipped with a CDD camera, serial Ca^{2+} images of fluo3 fluorescence in a single cardiomyocyte were registered (**a**) and relative fluorescence values [$(F - F_0)/F_0$] are illustrated as a function of time (**b**). The scale bar is 20 μm. Using an inverted microscope equipped with a Xenon lamp, fura2-AM preloaded cells were excited at 340 and 380 nm, and monitored at 510 nm. The corresponding 340/380 fluorescence ratios are illustrated in (**c**)

Results

Sorbitol induced-hyperosmotic stress elicits Ca^{2+} transients in cardiomyocytes

Increases of intracellular Ca^{2+} concentration ($[Ca^{2+}]i$) were visualized in single cardiomyocytes preloaded with fluo3-AM as relative fluorescence increases (Fig. 1a, b). Exposure of cardiomyocytes maintained in Ca^{2+}-containing Krebs buffer to sorbitol-induced hyperosmotic stress [600 mosmol (kg water)$^{-1}$] led to a small, fast Ca^{2+} increase that reached its maximum value at 12 ± 2 s

($n = 5$), followed by a much larger, delayed and slower $[Ca^{2+}]i$ increase that on average became oscillatory 356 ± 78 s ($n = 5$) after sorbitol addition (Fig. 1a, b). These increases in $[Ca^{2+}]i$ were also visualized in single cardiomyocytes preloaded with the ratiometric Ca^{2+} probe fura2-AM (Fig. 1c). Cardiomyocytes maintained in Ca^{2+}-containing Krebs buffer had a basal ratio of fura2-AM fluorescence (F340/F380) of 0.51 ± 0.03. Exposure of cardiomyocytes to sorbitol [600 mosmol (kg water)$^{-1}$] elicited a pattern of $[Ca^{2+}]i$ increase (Fig. 1c) similar to that observed with fluo3-AM (Fig. 1b). In the first 20 s after sorbitol addition the F340/F380 reached 0.84 ± 0.06 ($P < 0.001$ vs. basal), while in the next 20 s the F340/F380 ratio increased to 1.28 ± 0.12 ($P < 0.001$ vs. basal) (Fig. 1c). The fluorescence ratio continued increasing up to 250 s; however, after 4 h of sorbitol exposure, F340/F380 values returned to basal levels (data not shown). These results suggest that hyperosmotic stress induced a transient $[Ca^{2+}]i$ increase that lasted <4 h.

To determine whether the observed Ca^{2+} transients were triggered by hyperosmotic stress rather than by the osmolyte sorbitol itself, normo-osmotic [307 mosmol (kg water)$^{-1}$] sorbitol-containing Krebs buffer was prepared by replacing NaCl with sorbitol. This normo-osmotic sorbitol-containing solution did not induce the large and sustained Ca^{2+} transients produced by hyperosmotic sorbitol solutions (data not shown). These results suggest that sorbitol-induced hyperosmotic stress rather than sorbitol itself triggered the sustained oscillatory Ca^{2+} transients.

To further investigate the signaling pathways by which hyperosmotic stress elicits Ca^{2+} signals, cardiomyocytes maintained in Ca^{2+}-free Krebs buffer were exposed to sorbitol-induced hyperosmotic stress [600 mosmol (kg water)$^{-1}$]. This condition prevented the emergence of the large delayed oscillatory $[Ca^{2+}]i$ signal (Fig. 2a), strongly suggesting that this signal requires Ca^{2+} influx. The absence of extracellular calcium also decreased the initial Ca^{2+} signal component when was evaluated in fluo3-loaded cells, and totally abolished it in fura2-loaded cells (Supplementary Fig. 1). In cardiomyocytes maintained in Ca^{2+}-containing Krebs buffer, incubation with the phospholipase C (PLC) inhibitor U73122 (10 μM), the IP_3 receptor blocker xestospongin C (50 μM), the L-type Ca^{2+} channel inhibitor nifedipine (10 μM) or Cd^{2+} (100 μM) completely suppressed the sorbitol-induced large and oscillatory Ca^{2+} signal (Fig. 2b–e). The inhibitory effect of nifedipine suggests that hyperosmotic stress activates Ca^{2+} entry through L-type Ca^{2+} channels. The inhibitory effect of ryanodine (50 μM) (Fig. 2e) suggests that Ca^{2+}-induced Ca^{2+}-release via ryanodine receptor channels also contributes to the oscillatory Ca^{2+} increase produced by hyperosmotic stress.

Addition of 1 mM EGTA to the Ca^{2+}-containing Krebs buffer (i.e. 0.8 mM free Ca^{2+} as determined using the MaxChelator Winmaxc 2 software, Stanford University, CA), completely suppressed the large and oscillatory Ca^{2+} increase induced by hyperosmotic stress (Fig. 2g). Addition of the sarco/endoplasmic reticulum Ca^{2+}-ATPase (SERCA) inhibitor thapsigargin (1 μM) to cardiomyocytes preloaded with fluo3-AM and kept in Ca^{2+} free solution produced a slow increase in intracellular fluorescence that peaked at 300 s, and which is presumably due to Ca^{2+} loss from internal stores. Neither subsequent addition of caffeine (5 mM) nor exposure to sorbitol-induced hyperosmotic stress [600 mosmol (kg water)$^{-1}$] stimulated additional Ca^{2+} increases (Fig. 2h). Addition of 2 mM external Ca^{2+} to cells pre-incubated with thapsigargin did induce, however, a modest fluorescence signal increase (Fig. 2h). These results suggest that hyperosmotic stress induces Ca^{2+} release from thapsigargin-sensitive internal Ca^{2+} stores; the resulting store depletion triggers Ca^{2+} influx presumably through store operated Ca^{2+} entry channels. Addition of hyperosmotic sorbitol [600 mosmol (kg water)$^{-1}$] also induced a significant but slow depolarization of cardiomyocytes (Supplementary Fig. 2), which was too slow to cause massive Ca^{2+} entry but strong enough to increase the open probability of L-type channels.

In summary, these results suggest that the large and oscillatory Ca^{2+} increase produced by hyperosmotic stress involves the participation of Ca^{2+} influx through nifedipine and Cd^{2+}-sensitive Ca^{2+} channels, which probably correspond to L-type Ca^{2} channels, and of Ca^{2+} release from internal stores through ryanodine-sensitive and PLC-IP_3 dependent pathways.

Hyperosmotic stress promotes cardiomyocyte cell death through mitochondrial depolarization and metabolic collapse

An increase in $[Ca^{2+}]i$ can induce Ca^{2+} uptake by mitochondria. In order to detect if mitochondrial Ca^{2+} increases in response to the cytoplasmic Ca^{2+} signals, cardiomyocytes were preloaded with rhod2-AM (as a mitochondrial Ca^{2+} probe) and fluo3-AM (as a cytoplasmic Ca^{2+} probe). Sorbitol-induced hyperosmotic stress [600 mosmol (kg water)$^{-1}$] produced a significant mitochondrial Ca^{2+} increase a few minutes after sorbitol addition that paralleled the cytoplasmic increase (Fig. 3a). Interestingly, the delayed and oscillatory cytoplasmic Ca^{2+} increase induced by sorbitol was associated with a large but non-oscillatory mitochondrial Ca^{2+} increase (Fig. 3a). The magnitude of both the cytoplasmic and mitochondrial Ca^{2+} signals increased when increasing the osmolarity of the sorbitol solutions (Fig. 3b, c). Yet rhod2, the fluorescent probe used to detect mitochondrial Ca^{2+} signals, has high affinity for Ca^{2+} and saturates at high Ca^{2+} levels. This feature may

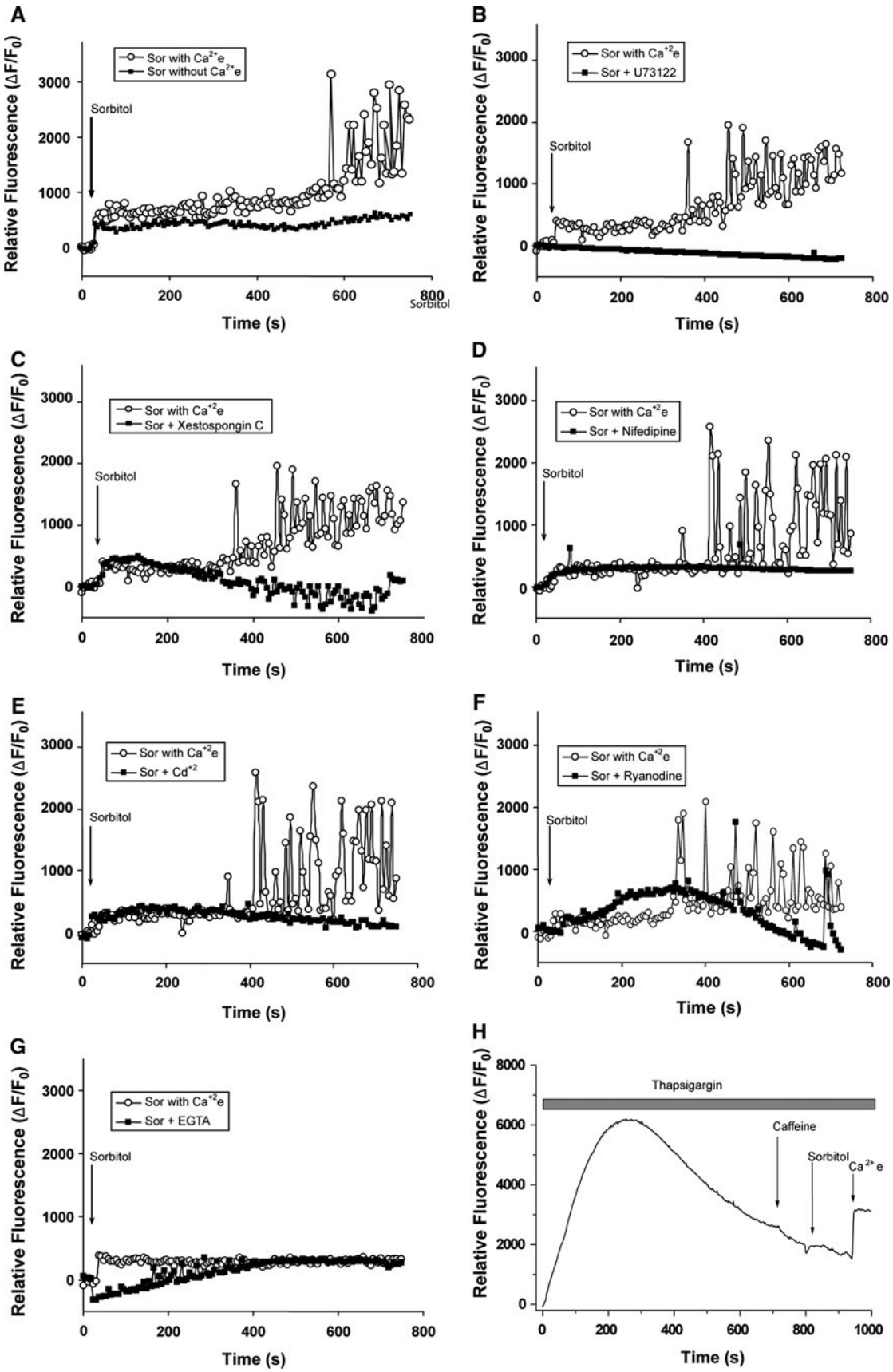
A
Relative Fluorescence (ΔF/F0)
Sor with Ca+2e
Sor without Ca2+e
Sorbitol
Time (s)
B
Sor with Ca+2e
Sor + U73122
C
Sor + Xestospongin C
D
Sor + Nifedipine
E
Sor + Cd+2
F
Sor + Ryanodine
G
Sor + EGTA
H
Thapsigargin
Caffeine
Ca2+e

◀ **Fig. 2** Effect of different agents on the intracellular Ca^{2+} increase induced by hyperosmotic stress. Cardiomyocytes, maintained in Ca^{2+}-free Krebs buffer (**a**) or Ca^{2+}-containing Krebs buffer (**b–g**), were preloaded with fluo3-AM and preincubated for 30 min with 10 μM U73122 (**b**), 100 μM xestospongin C (**c**), 10 μM nifedipine (**d**), 100 μM Cd^{2+} (**e**), 50 μM ryanodine (**f**) or 1 mM EGTA (**g**). Cells were then exposed to Ca^{2+}-containing Krebs buffer plus sorbitol [600 mosmol (kg water)$^{-1}$] at the time indicated with an *arrow*. (**h**) 1 μM thapsigargin was added to fluo3 preloaded cardiomyocytes in Ca^{2+}-free Krebs buffer, followed 12 min later by addition of 5 mM caffeine; 2 min later cardiomyocytes were stimulated with sorbitol [600 mosmol (kg water)$^{-1}$] and 2 min later, 2 mM extracellular Ca^{2+} (Ca^{2+}e) was added. Fluo3 fluorescence images were registered and relative fluorescence was calculated as above. All figures are representative of three experiments, analyzing 6–14 cells in each experiment. In percentage, the cells showing the displayed behavior for each agent tested were: U73122 = 100 ± 0%; U73343 = 86 ± 1%; xestospongin C = 84 ± 2%; nifedipine = 92 ± 1%; Cd^{2+} = 72 ± 8%; ryanodine = 68 ± 10% and EGTA = 64 ± 3%

explain why mitochondrial Ca^{2+} signals did not increase linearly with osmotic stress (Fig. 3c).

Mitochondrial depolarization is an immediate consequence of mitochondrial Ca^{2+} uptake [31]. In cardiomyocytes preloaded with tetramethylrhodamine methyl ester (TMRM, 100 nM) as a membrane potential probe, we observed by confocal microscopy that hyperosmotic stress induced significant mitochondrial depolarization in a dose-dependent manner (Fig. 3d–e). The highest mitochondrial depolarization was observed following addition of CCCP (10 μM) (Fig. 3d–e). Hyperosmotic stress-induced mitochondrial depolarization was completely dependent on Ca^{2+} influx because it was not observed in cardiomyocytes maintained in Ca^{2+}-free Krebs buffer (Fig. 3f). These results suggest that the degree of mitochondrial depolarization induced by different hyperosmotic solutions correlate directly with the hyperosmotic stress-dependent $[Ca^{2+}]$i, i.e. higher hyperosmotic stress conditions caused higher increases of cytoplasmic and mitochondrial Ca^{2+} and higher mitochondrial depolarization (Fig. 3b–e).

The depolarization of mitochondria may induce the opening of the mitochondrial permeability transition pore, releasing either the apoptosis-inducing factor (AIF) or cytochrome c [31]. Immunofluorescence analysis of cardiomyocytes revealed that under basal conditions AIF was present as a defined punctuated staining in the cytoplasm. Exposure of cardiomyocytes for up to 4 h to sorbitol-induced hyperosmotic stress [600 mosmol (kg water)$^{-1}$] did not modify AIF localization (Fig. 4a). Cytochrome c was also visualized by immunofluorescence as a defined punctuated staining in the cytoplasm, similar to that detected for AIF. Exposure of cardiomyocytes to hyperosmotic stress for 2 h, however, changed this punctuated pattern to diffuse staining (Fig. 4b). These combined results suggest that hyperosmotic stress induced the release of cytochrome c but not of AIF from the mitochondria.

Exposure of cardiomyocytes to hyperosmotic culture media [600 mosmol (kg water)$^{-1}$] increased the fragmentation of pro-caspases 9 and 3 (Fig. 4c) with a maximum at 2 h. Pro-caspase 9 fragmentation correlated with an increase of caspase 9 proteolytic activity (Fig. 4d). Yet, incubation of cardiomyocytes with the pan-caspase inhibitor Z-VAD-fmk, at a concentration that prevented caspase 3 activation (Supplementary Fig. 3), did not rescue cardiomyocytes from death (Fig. 4e), suggesting that hyperosmotic stress induces caspase-independent cell death. Moreover, preincubation of cardiomyocytes with cyclosporin A (CsA, 0.5 μM), an inhibitor of the mitochondrial permeability transition pore, did not protect cardiomyocytes from hyperosmotic stress-induced cell death, as determined by cell viability and DNA laddering assays (Supplementary Fig. 4). These results suggest that opening of the mitochondrial permeability transition pore does not participate of the cellular pathways that promote cardiomyocyte death in response to hyperosmotic stress.

Mitochondrial depolarization has been associated with a decrease in mitochondrial ATP synthesis [32]. Hyperosmotic stress [600 mosmol (kg water)$^{-1}$] induced a 25% decrease in total ATP content in cardiomyocytes after 2 h of incubation (Fig. 4f). This reduction of ATP content suggests that hyperosmotic stress induces cardiomyocyte death via a metabolic collapse, rather than through caspase-dependent apoptosis.

Taken together, these results strongly suggest that hyperosmotic stress-induced Ca^{2+} influx increases mitochondrial Ca^{2+} levels, which presumably contribute to induce mitochondrial depolarization. The ensuing decrease of ATP synthesis would subsequently lead to a reduction in intracellular ATP content, which would trigger caspase-independent cardiomyocyte death.

The role of extracellular Ca^{2+} in cardiomyocyte death induced by hyperosmotic stress

To assess the role of extracellular Ca^{2+} in hyperosmotic stress-induced cardiomyocyte death, different concentrations of EGTA were used to decrease extracellular $[Ca^{2+}]$. The cardiomyocyte culture media contains 1.8 mM Ca^{2+}. Addition of up to 1 mM EGTA (final concentration) to the culture media did not induce cardiomyocyte death, as determined by cell viability assays and DNA laddering. Hyperosmotic stress-induced apoptosis was prevented, however, by addition of 1 mM EGTA (approximately 0.8 mM free Ca^{2+}) but not of 0.5 mM EGTA (approximately 1.3 mM free Ca^{2+}) to the culture media (Fig. 5a, b). Higher concentrations of EGTA (2–10 mM final) induced cardiomyocyte apoptosis even in the absence of hyperosmotic stress (Fig. 5a, b).

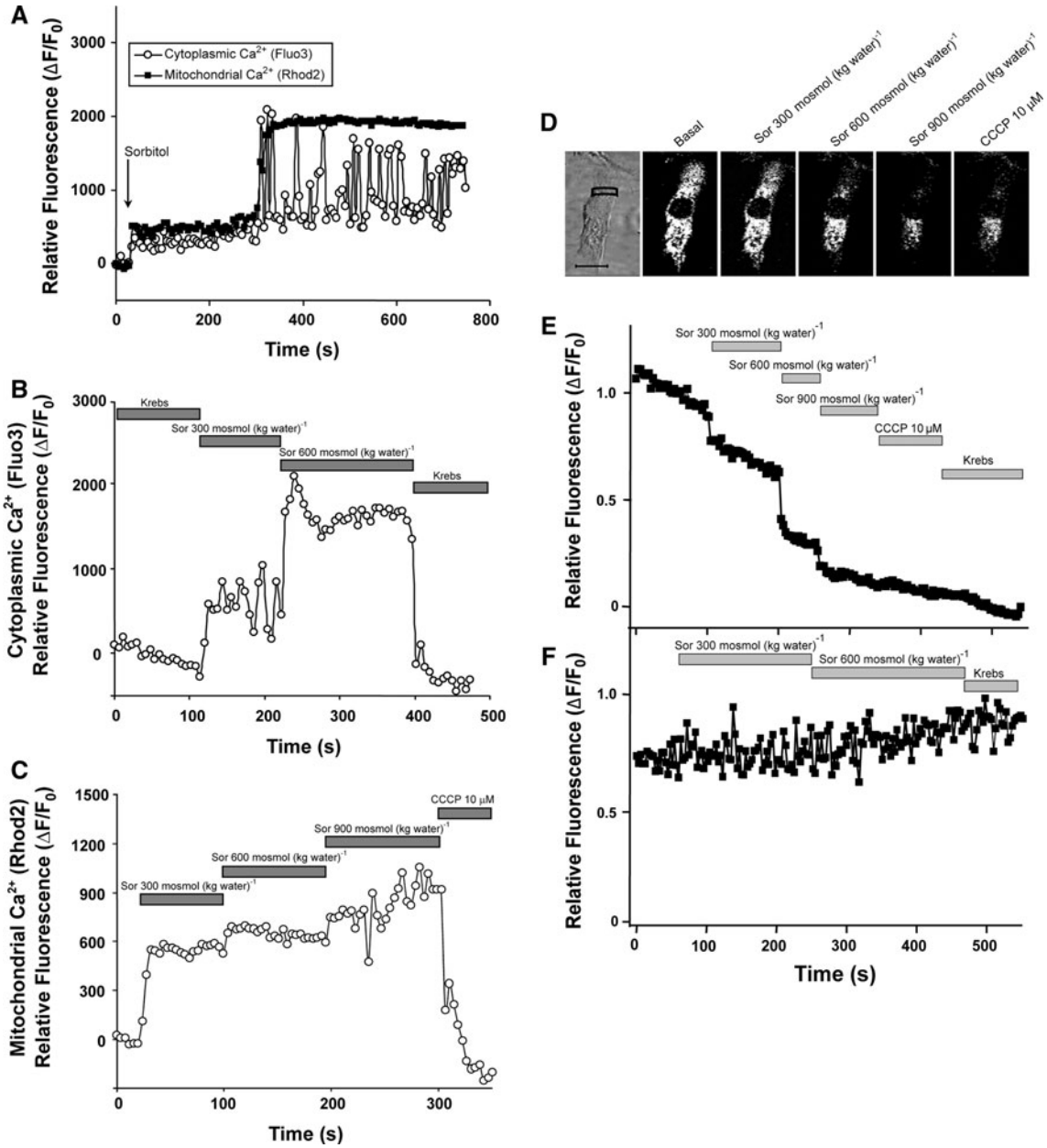

Fig. 3 Characterization of mitochondrial depolarization induced by hyperosmotic stress in cultured cardiomyocytes. (**a**) Cells maintained in Ca^{2+}-containing Krebs buffer were preloaded for 15 min at 4°C with rhod2-AM (5.4 μM) to determine mitochondrial Ca^{2+} (*black squares*) and then for 30 min at room temperature with fluo3-AM (5.4 μM) to determine cytoplasmic Ca^{2+} (*white circles*). Cells were washed and then stimulated at the time indicated with an *arrow* with culture media containing sorbitol [600 mosmol (kg water)$^{-1}$]. Fluorescent images were collected every 3–5 s with a multi channel configuration device (channel A for fluo3-AM, excitation 488 nm and emission 526 nm; channel B for rhod2-AM, excitation 543 nm and emission 580 nm). (**b**) Cells, maintained in Ca^{2+}-containing Krebs buffer were preloaded for 30 min at room temperature with fluo3-AM (5.4 μM) to determine cytoplasmic Ca^{2+}, washed and stimulated with Krebs buffer containing 300 or 600 mosmol (kg water)$^{-1}$ sorbitol as indicated in the figure. (**c**) Cells, maintained in Ca^{2+}-containing Krebs buffer were preloaded for 30 min at room temperature with rhod2-AM (5.4 μM) to determine mitochondrial Ca^{2+}, washed and stimulated with Krebs buffer containing 300, 600 or 900 mosmol (kg water)$^{-1}$ sorbitol as indicated in the figure. (**d**, **e**) Cells maintained in Ca^{2+}-containing Krebs buffer were preincubated with 100 nM TMRM and then exposed to Ca^{2+}-containing Krebs buffer supplemented with 300, 600 or 900 mosmol (kg water)$^{-1}$ sorbitol. Basal media osmolarity was 290 mosmol (kg water)$^{-1}$. The uncoupling agent CCCP (10 μM) was used to fully depolarize the mitochondria. Representative images of TMRM preloaded cardiomyocytes exposed to different hyperosmotic solutions are shown in (**c**). The scale bar is 10 μm. TMRM fluorescence was analyzed in the area defined on the cell shown in the transmitted light image. (**f**) Cells maintained in Ca^{2+}-free Krebs buffer and preincubated with 100 nM TMRM were exposed to Ca^{2+}-free media supplemented with 300 or 600 mosmol (kg water)$^{-1}$ sorbitol. Results are expressed as relative fluorescence $[(F - F_0)/F_0]$ and are representative of at least five independent experiments

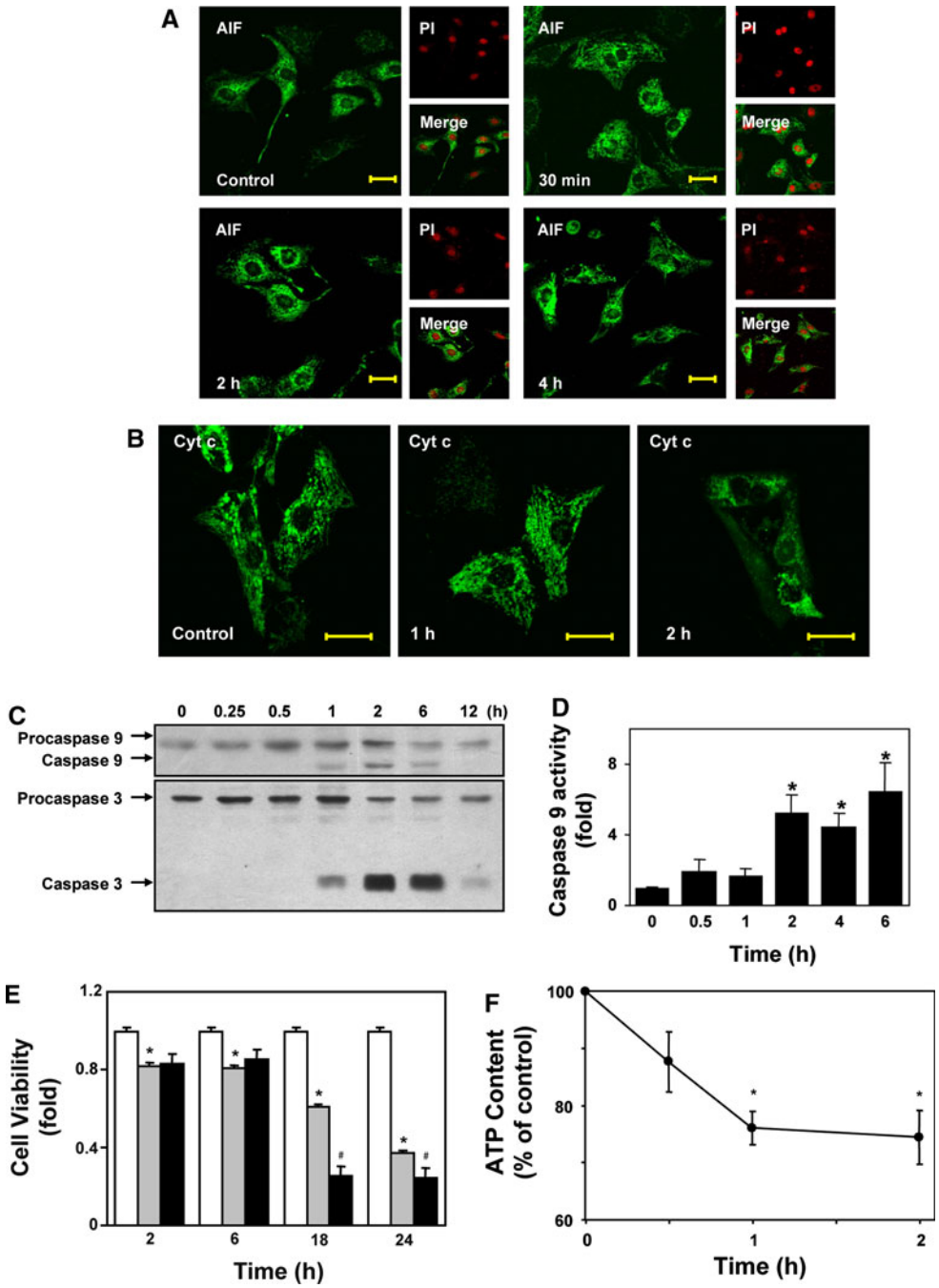

Fig. 4 Hyperosmotic stress triggered cardiomyocyte death, caspase cascade activation and reduced ATP content in cultured cardiomyocytes. Cardiomyocytes cultured in coverslips were exposed to culture media containing sorbitol [600 mosmol (kg water)$^{-1}$] and at the indicated times cells were fixed, blocked with bovine seroalbumin, incubated with anti apoptosis inducing factor (AIF) antibody (**a**) or anti cytochrome c (Cyt c) antibody (**b**) and revealed with anti mouse IgG-Alexa488. Nuclei were stained with propidium iodide (PI). Cells were exposed to hyperosmotic culture media [600 mosmol (kg water)$^{-1}$ sorbitol] and at different times, total protein extracts were prepared. (**c**) Procaspases and caspases 9 and 3 were detected by western blot analysis. Gels are representative of five different experiments. (**d**) Caspase 9 activity was measured using Ac LEHD-pNA. (**e**) Cardiomyocytes were incubated with culture media (control, white bars), sorbitol (600 mosmol (kg water)$^{-1}$, gray bars) or sorbitol supplemented with the pan-caspase inhibitor Z-VAD-fmk (10 μM, *black bars*). At different times, viable cells were quantified as described in Materials and methods. (**f**) Total ATP content was measured using the luciferin/luciferase reaction as described in Materials and methods. Results are given as mean ± SEM for four independent experiments. * $P < 0.05$ versus 0 min, # $P < 0.005$ versus sorbitol. The scale bar is 20 μm

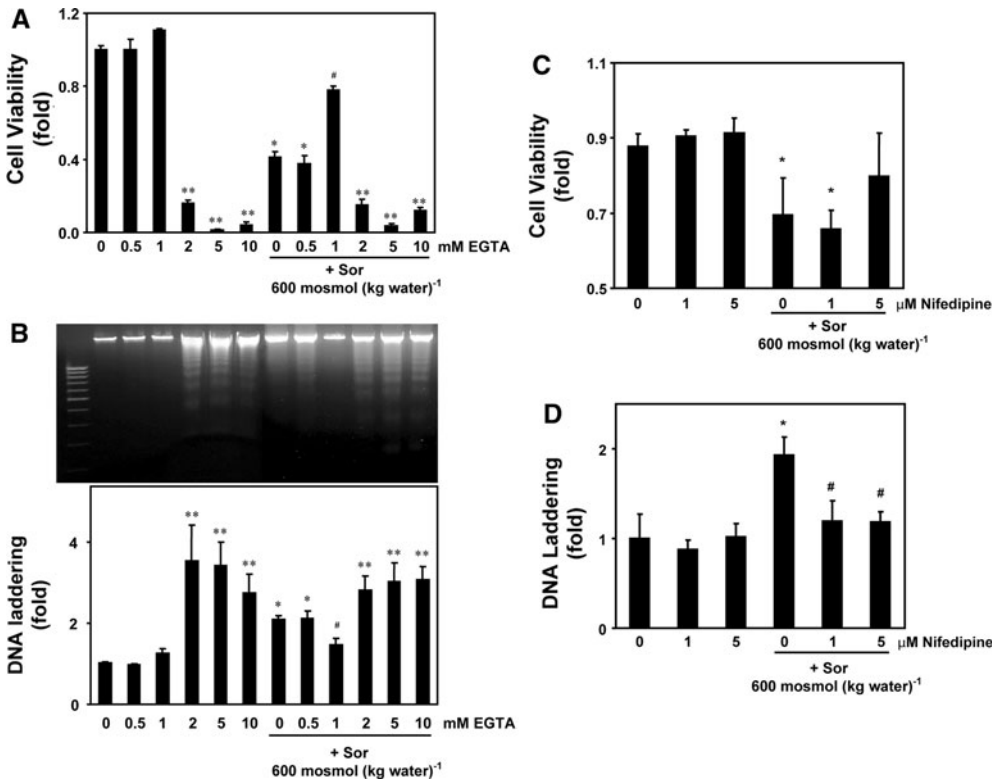

Fig. 5 Participation of extracellular Ca^{2+} in hyperosmotic stress-induced apoptosis in cultured cardiomyocytes. Cells were incubated for 24 h in DME:199 (4:1) containing 0–10 mM EGTA with or without 600 mosmol (kg water)$^{-1}$ sorbitol (Sor). (**a**) Cell viability was determined by the trypan blue exclusion method. (**b**) DNA extracted using the chloroform:phenol method was fractionated by electrophoresis in 2% agarose gels and visualized by ethidium bromide/UV. The standard corresponds to 100 bp DNA ladder. Results are given as mean ± SEM of four independent experiments. * $P < 0.05$ versus control (0 mM EGTA without sorbitol); ** $P < 0.01$ versus control; $^{\#}$ $P < 0.05$ versus 0 mM EGTA plus 600 mosmol (kg water)$^{-1}$ sorbitol. Cells were preincubated for 30 min with 1 or 5 μM nifedipine and then exposed for 24 h to DME:199 (4:1) supplemented with or without 600 mosmol (kg water)$^{-1}$ sorbitol (Sor). (**c**) shows cell viability and (**d**) shows DNA laddering. Results are given as mean ± SEM of three independent experiments. * $P < 0.05$ versus control 0 μM nifedipine; $^{\#}$ $P < 0.05$ versus 0 μM nifedipine plus 600 mosmol (kg water)$^{-1}$ sorbitol

In order to assess the role of the sorbitol-induced large and oscillatory Ca^{2+} increase on viability and DNA laddering, cardiomyocytes were pre-incubated 30 min with 1 or 5 μM nifedipine and then exposed to 600 mosmol (kg water)$^{-1}$ sorbitol. A significant decrease in hyperosmotic stress-induced DNA laddering was observed in these conditions. However, no change in the hyperosmotic-induced cardiomyocyte death was detected (Fig. 5c, d).

The association between mitochondrial Ca^{2+} increase and reduction of ATP content was assessed using 1 mM EGTA and ruthenium red (RuRed) to inhibit the mitochondrial Ca^{2+} uniporter [33]. Both compounds completely suppressed the mitochondrial Ca^{2+} increase produced by hyperosmotic stress (Fig. 6a, b). EGTA and RuRed also prevented the hyperosmotic stress-induced reduction in ATP content (Fig. 6c). These results, suggest that the reduction in ATP content, hence cell viability, was due to the mitochondrial collapse induced by mitochondrial Ca^{2+} increase.

The transcription factor CREB is activated by hyperosmotic stress and is involved in cell survival

We next assessed the participation of CREB as a potential Ca^{2+}-dependent transcription factor involved in cardiomyocyte survival. Hyperosmotic stress induced by sorbitol [600 mosmol (kg water)$^{-1}$] increased significantly CREB phosphorylation (9.6 ± 0.6 fold) after 10 min of incubation (Fig. 7a). EMSA assays indicated that hyperosmotic stress induced CREB DNA binding activity after 0.5 h (Fig. 7b). Supershift analysis showed that the protein-DNA complex corresponded to CREB (Fig. 7c). Addition of 100-fold excess of non-radioactive oligonucleotide, but not of a mutant form of the CRE consensus sequence, specifically displaced the radioactive oligonucleotide bound to CREB, confirming the specificity of the assay (Fig. 7c). The MEK-1 inhibitor PD98059 (PD), the p38-MAPK inhibitor SB203580 (SB) and BAPTA-AM all inhibited hyperosmotic stress-dependent CREB phosphorylation; in contrast, the PI3-K inhibitor LY294002 (LY), the

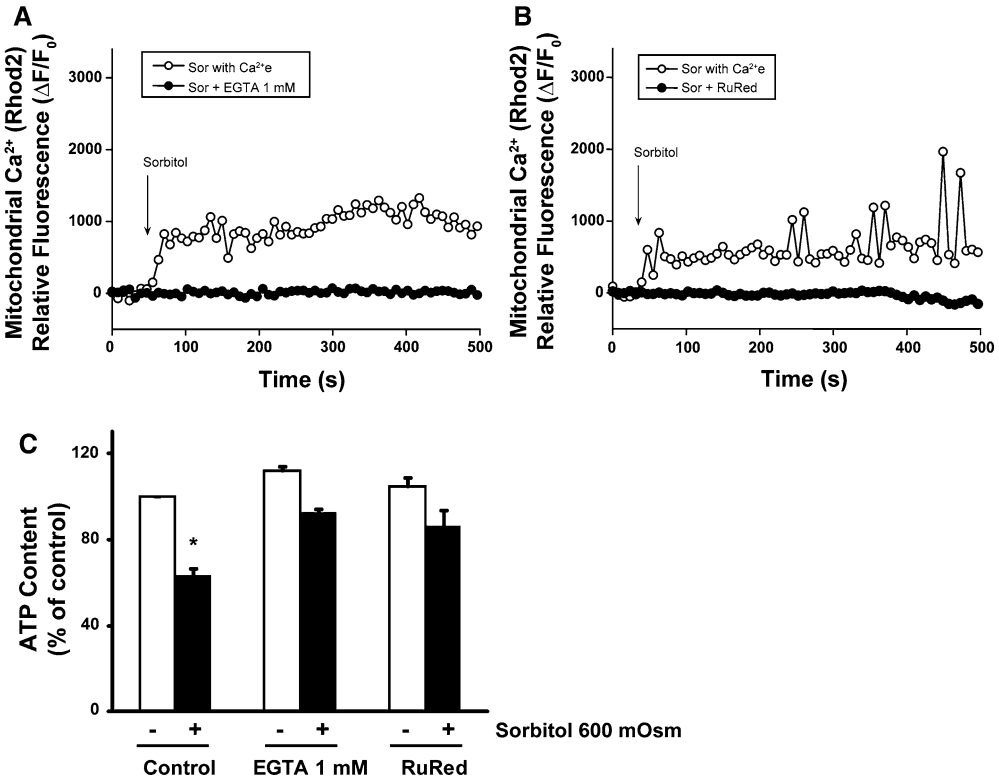

Fig. 6 Mitochondrial Ca^{2+} increase and reduction of ATP content induced by hyperosmotic stress. Cardiomyocytes, maintained in Ca^{2+}-containing Krebs buffer, were preloaded with rhod2-AM (5.4 μM) for 30 min at room temperature and preincubated for 30 min with 1 mM EGTA (**a**) or ruthenium red (RuRed, 1 μM) (**b**) Cells were then exposed to Ca^{2+}-containing Krebs buffer plus sorbitol [600 mosmol (kg water)$^{-1}$] at the time indicated with an *arrow*. Fluorescent images were collected every 5 s in a confocal microscopy (excitation 543 nm and emission 580 nm). (**c**) Total ATP content was measured using the luciferin/luciferase reaction as described in Materials and methods. Results are given as mean ± SEM for four independent experiments. * $P < 0.05$ versus control without sorbitol

calmodulin kinase II inhibitor KN62, and the calcineurin inhibitor CsA had no effect (Fig. 7d). These results indicate that hyperosmotic stress stimulates CREB phosphorylation via Ca^{2+}-dependent pathways that include ERK and p38-MAPK, and rule out the participation of PI3-K, calmodulin kinase II and calcineurin on this activation.

To evaluate CREB participation in the survival of cardiomyocytes upon exposure to hyperosmotic stress, cells were transduced with an adenovirus overexpressing dominant negative CREB (Ad dnCREB) and incubated with culture media containing 600 mosmol (kg water)$^{-1}$ sorbitol in the presence and absence of 1 mM EGTA. Levels of dnCREB expression were verified by Western blot analysis (Supplementary Fig. 5). A *β*-galactosidase overexpressing adenovirus (Ad LacZ) was used as control. Hyperosmotic stress induced cardiomyocyte apoptosis in Ad dnCREB and Ad LacZ transduced cardiomyocytes maintained in non-EGTA containing culture media, as evidenced by cell viability and DNA laddering (Fig. 8a, b). Yet, Ad dnCREB but not Ad LacZ abolished the anti-apoptotic effect of 1 mM EGTA (Fig. 8a, b). These results suggest that CREB is directly involved in the Ca^{2+}-dependent survival pathways triggered by hyperosmotic stress.

Discussion

Calcium plays important roles in cardiomyocytes, regulating not only the relaxation–contraction process but also controlling gene expression [34]. Here, we showed that Ca^{2+} is also an important mediator in hyperosmotic stress-induced cardiomyocyte survival and death. Osmotic alterations in the heart during ischemia and reperfusion, diabetic coma and septic shock have been described [5]. We demonstrated here that cardiomyocytes maintained in Ca^{2+}-containing Krebs–Ringer solution display large and oscillatory Ca^{2+} signals in response to hyperosmotic stress. The Ca^{2+} ratiometric probe fura2 yielded a basal F340/F380 ratio of 0.51 ± 0.03 for cardiomyocytes maintained in Ca^{2+}-containing Krebs buffer. Using in vitro Ca^{2+} calibration buffers, this ratio corresponds to 102 ± 9 nM [Ca^{2+}]. This value is in agreement with previous basal [Ca^{2+}] values described for neonatal rat ventricular cardiomyocytes [35, 36].

Hyperosmotic stress prompts a 30% decrease in cardiomyocyte volume [10]. Our data show that stimulation induced a fast but discrete Ca^{2+} increase that required Ca^{2+} influx from the extracellular medium and PLC

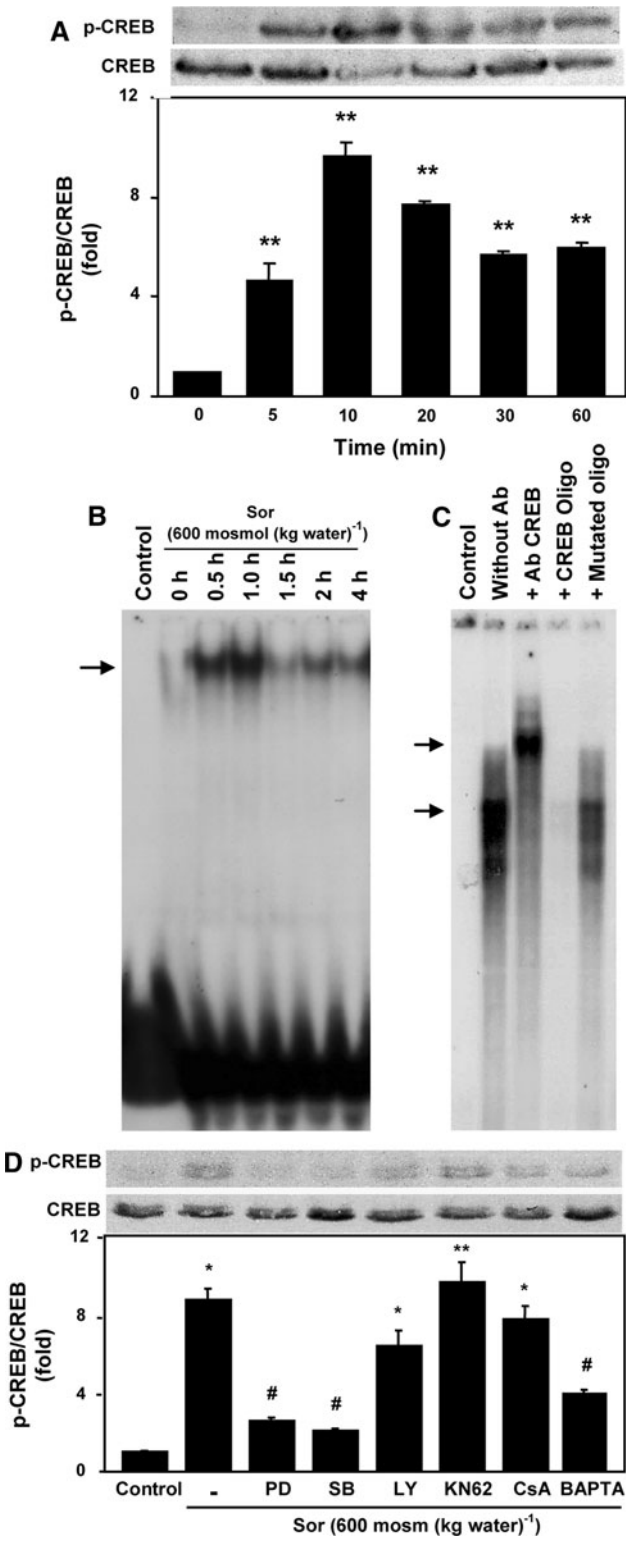

Fig. 7 Activation of CREB by hyperosmotic stress in cultured cardiomyocytes. Cells were exposed to culture media containing sorbitol [600 mosmol (kg water)$^{-1}$]. At the indicated times, total protein extracts or nuclear and cytoplasmic protein extracts were prepared. (**a**) Phosphorylated CREB (P-CREB) and total CREB levels were determined by western blot using anti phospho-CREB (p-CREB) or anti CREB polyclonal antibodies, respectively. (**b**) Nuclear extracts were obtained from cardiomyocytes incubated in isosmotic solution (control), or from cardiomyocytes exposed to hyperosmotic stress [600 mosmol (kg water)$^{-1}$ sorbitol] for 0.5, 1, 1.5, 2 or 4 h. *Lane 1* corresponds to a control without nuclear extract. EMSA was performed as indicated in Materials and methods. (**c**) Nuclear extracts were obtained from control cardiomyocytes or from cells exposed for 1 h to hyperosmotic stress (600 mosmol (kg water)$^{-1}$ sorbitol). Supershift assays were performed using anti CREB antibody as described in Materials and methods. 100-fold excess of non-radioactive CRE oligonucleotide (CRE oligo) or 100-fold excess of a mutant CRE oligonucleotide (mutated oligo) were used as controls. (**d**) Cardiomyocytes were preincubated for 30 min with 50 μM PD98059 (PD, MEK-1 inhibitor), 10 μM SB203580 (SB, p38-MAPK inhibitor), 50 μM LY294002 (LY, PI3-K inhibitor), 1 μM KN62 (calmodulin kinase inhibitor), 0.5 μM cyclosporin A (CsA, calcineurin inhibitor) or 100 mM BAPTA-AM (BAPTA, intracellular Ca^{2+} chelating agent) and then incubated under hyperosmotic stress conditions [600 mosmol (kg water)$^{-1}$ sorbitol] for 10 min. Results are given as mean ± SEM ($n = 3$). Gels are representative of three independent experiments. * $P < 0.05$ and ** $P < 0.01$ versus control or $t = 0$ min; $^{\#}$ $P < 0.05$ versus 600 mosmol (kg water)$^{-1}$ sorbitol

activity. Noteworthy, PLC activity and IP3 have been associated with the stimulation of mechanosensitive Ca^{2+} channels such as TRPV4 [37, 38], suggesting that cell shrinkage induced by hyperosmotic stress might activate PLC-dependent mechanosensitive Ca^{2+} channels, that mediate the initial Ca^{2+} influx component.

The slow, large and oscillatory Ca^{2+} increase induced by hyperosmotic stress requires Ca^{2+} influx through L-type Ca^{2+} channels, plus Ca^{2+} release from thapsigargin and caffeine-sensitive internal stores. Hyperosmotic stress did not induce large Ca^{2+} transients in cardiomyocytes pre-treated with xestospongin C or U73122, suggesting that Ca^{2+} influx is not sufficient by itself to generate these signals. However, Ca^{2+} influx through L-type Ca^{2+} channels can trigger Ca^{2+} release from internal stores by stimulating PLC-dependent IP_3 generation, which through subsequent stimulation of ryanodine receptor-mediated Ca^{2+}-induced Ca^{2+} release (CICR), would generate the observed large and delayed Ca^{2+} transients. This proposed sequence of events would explain the inhibitory effects of nifedipine, xestospongin C, U73122 and ryanodine (Fig. 9). Therefore, the Ca^{2+} oscillations observed in cardiomyocytes exposed to hyperosmotic stress may arise from cyclic Ca^{2+} release-and-uptake processes. Such Ca^{2+} oscillations are involved in a wide variety of cellular functions [39, 40]. As a general rule, Ca^{2+} entry through voltage-gated channels in electrically excitable cells [41] activates PLC and the production of IP_3. IP_3 induces Ca^{2+} release from the endoplasmic reticulum, which promotes ryanodine receptor-mediated CICR, and gives rise to Ca^{2+} oscillations [39, 40, 42].

Recent reports have shown that an increase in $[Ca^{2+}]i$ in the vicinity of mitochondria results in significant mitochondrial $[Ca^{2+}]$ uptake [43]. The ensuing rise of intra

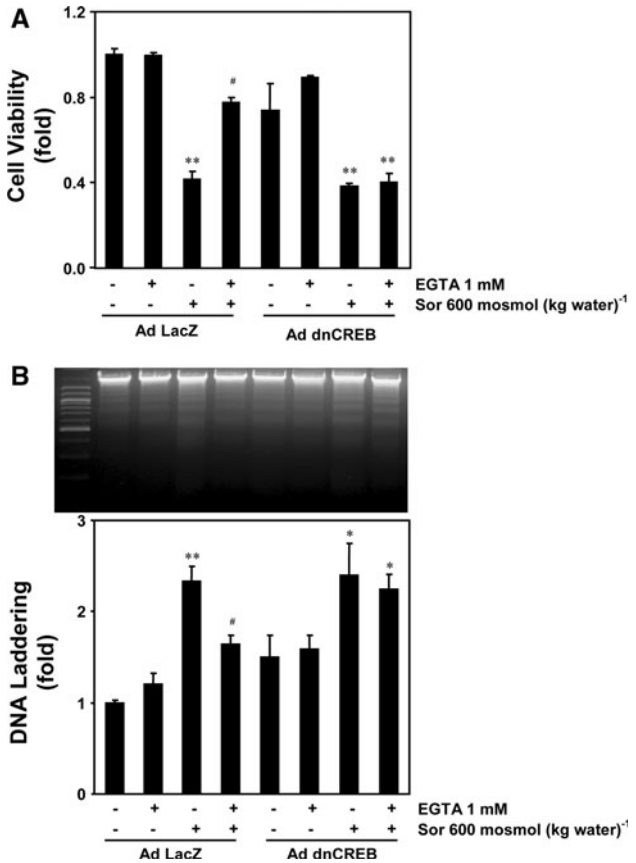

Fig. 8 Participation of CREB in hyperosmotic stress-induced survival pathways in cultured cardiomyocytes. Cells were transduced with an adenovirus overexpressing dominant negative CREB (Ad dnCREB at MOI 300). An adenovirus overexpressing LacZ was used as control (Ad LacZ). Cells were incubated for 24 h in DME:199 (4:1) containing 0–10 mM EGTA with or without 600 mosmol (kg water)$^{-1}$ sorbitol (Sor). (**a**) Cell viability was determined by the trypan blue exclusion method. (**b**) DNA was extracted using the chloroform:phenol method, fractionated by electrophoresis in 2% agarose gels and visualized by ethidium bromide/UV. The standard corresponds to 100 bp DNA ladder. Results are given as mean ± SEM of four independent experiments. * $P < 0.05$ versus respective control (0 mM EGTA without sorbitol); ** $P < 0.01$ versus respective control; # $P < 0.05$ versus Ad LacZ plus 0 mM EGTA plus 600 mosmol (kg water)$^{-1}$ sorbitol

mitochondrial [Ca^{2+}] triggers mitochondrial depolarization, which produces a decrease in ATP synthesis that finally ends in cell death (Fig. 9). Our results show that in cardiomyocytes this process can be suppressed by reducing extracellular Ca^{2+}, since hyperosmotic stress did not induce mitochondrial depolarization when lowering extracellular Ca^{2+} levels with 1 mM EGTA.

Mitochondrial Ca^{2+} uptake is an integral part of cellular Ca^{2+} signaling, actively participating in Ca^{2+} storage [44, 45]. Mitochondria take up Ca^{2+} from the cytoplasm through an uniporter, and release it through several different mechanisms [46]. However, an increase in mitochondrial [Ca^{2+}] can also trigger apoptosis through the permeabilization of the outer mitochondrial membrane. Several agents trigger apoptosis through activation of the Ca^{2+}-mediated mitochondrial permeability transition pore in various cell types. Such agents include Ca^{2+} ionophores and thapsigargin, neurotoxins, chemotherapeutics and pro-oxidants (for example, arachidonic acid and peroxynitrite) [46–48].

Recently, we described that mitochondria play a major role in the lethal response of HTC116 and HeLa cells to hyperosmotic stress [49]. Both cell types display mitochondrial dysfunction when exposed to hyperosmotic stress induced by sorbitol [600 mosmol (kg water)$^{-1}$], with loss of mitochondrial transmembrane potential, increased reactive oxygen species generation, and partial permeabilization of the outer mitochondrial membrane leading to AIF release. Importantly, in HCT116 cells such mitochondrial changes are caspase-independent, while in HeLa cells the process is caspase-dependent [49]. Moreover, a mitochondrion-targeted Bcl-2 mutant confers strong cytoprotection against cell death induced by hypertonic stress [49]. Our present data show that hyperosmotic stress-induced cardiomyocyte death is a caspase-independent process, resembling what occurs in HCT116 cells.

Several reports have described that when cells undergo apoptosis by mitochondrial outer membrane permeabilization, followed by caspase activation promoted by cytochrome c release, the use of caspase inhibitors fails to rescue cells from death [50]. Here, we observed that inhibition of caspase by Z-VAD treatment did not prevent hyperosmotic stress-induced cell death and rather increased sorbitol-induced mortality. These findings are consistent with previous reports in which Z-VAD enhances caspase-independent cell death modalities [51–53]. Thus, this "caspase-independent cell death" may occur as a consequence of mitochondrial failure and/or release of apoptotic agents from the mitochondria, such as AIF [49, 54]. In our model, we observed that preincubation of cardiomyocytes with CsA 0.5 μM, a concentration that inhibits the opening of the mitochondrial permeability transition pore in cultured cardiomyocytes [55], did not protect cardiomyocytes against hyperosmotic stress-induced cell death. Moreover, AIF release by hyperosmotic stress was not detected. An alternative possibility is that cells die due to the collapse of mitochondrial function. Supporting this last hypothesis, Colell et al. [50] described that increased ATP levels through the activation of glyceraldehyde-3-phosphate dehydrogenase, hence glycolysis, and enhanced autophagy cooperate to protect cells from caspase-independent cell death. Here, we described that hyperosmotic stress induced a 25% reduction of total ATP content in cardiomyocytes. Such reduction could be explained by a decrease in ATP synthesis due to the activation of the polyol pathway, but also by the collapse of mitochondrial function. The

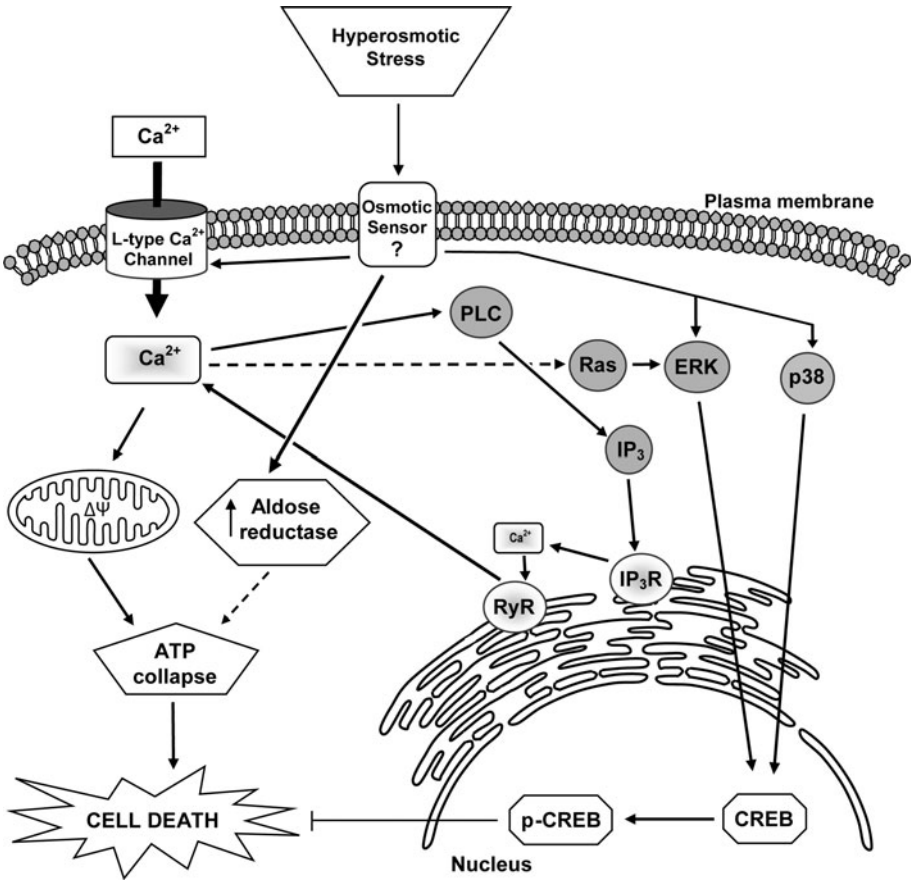

Fig. 9 Proposed mechanism for the generation of Ca^{2+} transients by sorbitol-dependent hyperosmotic stress and its relationship to cardiomyocyte death and survival. *PLC* phospholipase C; *IP_3* inositol-1,4,5-trisphosphate; *IP_3R* IP_3 receptor; *RyR* ryanodine receptor type 2; *ERK* extracellular signal-regulated kinase; *p38* p38-mitogen activated protein kinase; *CREB* cAMP responsive element binding protein

mitochondrial Ca^{2+} increase induced by hyperosmotic stress was prevented by previous addition of 1 mM EGTA to the culture media, as well as by pre-incubation with the mitochondrial uniporter inhibitor RuRed. Elimination of the mitochondrial Ca^{2+} increase significantly reduced the ATP content decrease caused by hyperosmotic stress. These results suggest that hyperosmotic stress sequentially induces Ca^{2+} influx, mitochondrial Ca^{2+} increase, reduction in ATP content and, finally, cell death.

The polyol pathway consists of two enzymes: aldose reductase, which reduces glucose to sorbitol with the aid of its cofactor NADPH, and sorbitol dehydrogenase with its cofactor NAD^+, which converts sorbitol to fructose. In cardiomyocytes, hyperosmotic stress activates the polyol pathway and induces intracellular sorbitol accumulation, a compatible osmolyte required for cell volume restoration upon a hypertonic challenge [10]. During polyol pathway activation, the lactate/pyruvate ratio (a measure of cytoplasmic redox state given by NADH/NAD) is increased [56, 57]. Hwang et al. proposed that increases in the lactate/pyruvate ratio could be explained by the flux of substrate through sorbitol dehydrogenase (which uses NAD^+) [56]. By competing for NAD^+, however, increases in flux via sorbitol dehydrogenase may decrease flux via glyceraldehyde-3-phosphate dehydrogenase, and thus reduce ATP synthesis by glycolysis [56, 57]. The involvement of the polyol pathway is further supported by the observation that inhibition of aldose reductase by zopolrestat rescued cardiomyocytes from hyperosmotic stress induced death [10]. Therefore, cardiomyocyte death induced by hyperosmotic stress could be explained by a metabolic collapse due to ATP reduction (Fig. 9).

We have shown that the complete absence of extracellular Ca^{2+} induces cardiomyocyte apoptosis. Culturing cardiomyocytes in Ca^{2+}-free medium, obtained by the addition of >2 mM EGTA to culture media containing 1.8 mM Ca^{2+}, induced cardiomyocyte death with DNA laddering. Therefore, extracellular Ca^{2+} concentrations equal or higher than 0.8 mM are required to maintain cardiomyocyte viability, probably through the activation of Ca^{2+}-dependent survival pathways.

Surprisingly, the addition of 1 mM EGTA, resulting in approximately 0.8 mM free Ca^{2+} in the culture media, prevented the hyperosmotic stress-induced cardiomyocyte apoptosis. This result can be explained by two possibilities: a) the decrease in Ca^{2+} availability due to EGTA chelation, which abolished the large and oscillatory Ca^{2+} signal and prevented or reduced mitochondrial depolarization; and b) the activation of Ca^{2+}-dependent survival signaling pathways. The first possibility agrees with the observation that

addition of 1 mM EGTA to obtain 0.8 mM free Ca^{2+}, completely abolished the large and oscillatory Ca^{2+} signal. The second possibility is in accordance with the fact that hyperosmotic stress promoted the activation of the transcription factor CREB, which has been associated with cell survival in neurons and cancer cells [58–60]. CREB mediates survival by enhancing transcription of anti-apoptotic bcl-2 family members [61, 62]. Recently we showed that IGF-1, a pro-hypertrophy anti-apoptotic peptide hormone, activates CREB in cardiomyocytes and mediates its anti-apoptotic effects [63]. Moreover, CREB is activated by Ca^{2+}-dependent signaling pathways [64, 65]. We observed a small increase in $[Ca^{2+}]i$ after exposure of cardiomyocytes maintained in 1 mM EGTA to hyperosmotic stress. This small Ca^{2+} increase could be responsible for hyperosmotic stress-induced CREB phosphorylation, because BAPTA, an intracellular Ca^{2+} chelating agent, completely suppressed CREB activation. The inactivation of CREB by overexpression of a dominant negative CREB completely suppressed the anti-apoptotic effect of 1 mM EGTA in cardiomyocytes exposed to hyperosmotic stress. These results suggest therefore, that the anti-apoptotic effects caused by the addition of 1 mM EGTA are due in part to CREB activation (Fig. 9).

In summary, our results show that Ca^{2+} plays a dual role in the response of cardiomyocytes to hyperosmotic stress. Intracellular Ca^{2+} transients induced by hyperosmotic stress trigger pro-apoptotic signals mediated by Ca^{2+} overload and the ensuing collapse of mitochondrial function, and simultaneously, Ca^{2+} promotes the activation of CREB as a pro-survival transcription factor.

Acknowledgments We thank Fidel Albornoz and Ruth Marquez for their technical assistance and Drs Paola Llanos and David Mears (Faculty of Medicine, Universidad de of Chile, Santiago, Chile) for their help with fura2-AM experiments. This work was supported by FONDAP (Fondo de Areas Prioritarias, Fondo Nacional de Desarrollo Cientifico y Tecnologico, CONICYT, Chile) grant 15010006 (to S. L., C. H., E. J.). We also thank the International Collaboration Program ECOS-CONICTY grants C04B03 and C08S01 (to G. K. and S. L.) and FONDECYT Postdoctoral Grant 3070043 (to V. E.). C. M., C. I., V. P., R. B., C. Q., A. C. and J. M. V. are recipients of Ph. D. fellowships from CONICYT, Chile. S. L. is in a sabbatical leave at The University of Texas Southwestern Medical Center, Dallas.

Conflicts of interest statement The authors declare that they have no conflict of interest.

References

1. Davies MJ (2000) The cardiomyopathies: an overview. Heart 83:469–474
2. Bing OH (1994) Hypothesis: apoptosis may be a mechanism for the transition to heart failure with chronic pressure overload. J Mol Cell Cardiol 26:943–948
3. Olivetti G, Abbi R, Quaini F, Kajstura J, Cheng W, Nitahara JA, Quaini E, Di Loreto C, Beltrami CA, Krajewski S, Reed JC, Anversa P (1997) Apoptosis in the failing human heart. N Engl J Med 336:1131–1141
4. Galvez A, Morales MP, Eltit JM, Ocaranza P, Carrasco L, Campos X, Sapag-Hagar M, Diaz-Araya G, Lavandero S (2001) A rapid and strong apoptotic process is triggered by hyperosmotic stress in cultured rat cardiac myocytes. Cell Tissue Res 304:279–285
5. Wright AR, Rees SA (1998) Cardiac cell volume: crystal clear or murky waters? A comparison with other cell types. Pharmacol Ther 80:89–121
6. Hoover HE, Thuerauf DJ, Martindale JJ, Glembotski CC (2000) Alpha B-crystallin gene induction and phosphorylation by MKK6-activated p38. A potential role for alpha B-crystallin as a target of the p38 branch of the cardiac stress response. J Biol Chem 275:23825–23833
7. Takatani T, Takahashi K, Uozumi Y, Shikata E, Yamamoto Y, Ito T, Matsuda T, Schaffer SW, Fujio Y, Azuma J (2004) Taurine inhibits apoptosis by preventing formation of the Apaf-1/caspase-9 apoptosome. Am J Physiol 287:C949–C953
8. Takatani T, Takahashi K, Uozumi Y, Matsuda T, Ito T, Schaffer SW, Fujio Y, Azuma J (2004) Taurine prevents the ischemia-induced apoptosis in cultured neonatal rat cardiomyocytes through Akt/caspase-9 pathway. Biochem Biophys Res Commun 316:484–489
9. Burg MB, Kwon ED, Kultz D (1997) Regulation of gene expression by hypertonicity. Annu Rev Physiol 59:437–455
10. Galvez AS, Ulloa JA, Chiong M, Criollo A, Eisner V, Barros LF, Lavandero S (2003) Aldose reductase induced by hyperosmotic stress mediates cardiomyocyte apoptosis—differential effects of sorbitol and mannitol. J Biol Chem 278:38484–38494
11. Distelhorst CW, Shore GC (2004) Bcl-2 and calcium: controversy beneath the surface. Oncogene 23:2875–2880
12. Hanson CJ, Bootman MD, Roderick HL (2004) Cell signalling: IP3 receptors channel calcium into cell death. Curr Biol 14:R933–R935
13. Kruman I, Guo Q, Mattson MP (1998) Calcium and reactive oxygen species mediate staurosporine-induced mitochondrial dysfunction and apoptosis in PC12 cells. J Neurosci Res 51:293–308
14. Lynch K, Fernandez G, Pappalardo A, Peluso JJ (2000) Basic fibroblast growth factor inhibits apoptosis of spontaneously immortalized granulosa cells by regulating intracellular free calcium levels through a protein kinase Cdelta-dependent pathway. Endocrinology 141:4209–4217
15. Martikainen P, Kyprianou N, Tucker RW, Isaacs JT (1991) Programmed death of nonproliferating androgen-independent prostatic cancer cells. Cancer Res 51:4693–4700
16. Tombal B, Denmeade SR, Isaacs JT (1999) Assessment and validation of a microinjection method for kinetic analysis of $[Ca^{2+}]i$ in individual cells undergoing apoptosis. Cell Calcium 25:19–28
17. Zirpel L, Lippe WR, Rubel EW (1998) Activity-dependent regulation of $[Ca^{2+}]i$ in avian cochlear nucleus neurons: roles of protein kinases A and C and relation to cell death. J Neurophysiol 79:2288–2302
18. Jiang S, Chow SC, Nicotera P, Orrenius S (1994) Intracellular Ca^{2+} signals activate apoptosis in thymocytes: studies using the Ca^{2+}-ATPase inhibitor thapsigargin. Exp Cell Res 212:84–92
19. Pinton P, Ferrari D, Magalhaes P, Schulze-Osthoff K, Di Virgilio F, Pozzan T, Rizzuto R (2000) Reduced loading of intracellular Ca^{2+} stores and downregulation of capacitative Ca^{2+} influx in Bcl-2-overexpressing cells. J Cell Biol 148:857–862
20. Wertz IE, Dixit VM (2000) Characterization of calcium release-activated apoptosis of LNCaP prostate cancer cells. J Biol Chem 275:11470–11477

21. Bito H, Takemoto-Kimura S (2003) Ca(2+)/CREB/CBP-dependent gene regulation: a shared mechanism critical in long-term synaptic plasticity and neuronal survival. Cell Calcium 34:425–430
22. Persengiev SP, Green MR (2003) The role of ATF/CREB family members in cell growth, survival and apoptosis. Apoptosis 8: 225–228
23. Brindle PK, Montminy MR (1992) The CREB family of transcription activators. Curr Opin Genet Dev 2:199–204
24. Deisseroth K, Mermelstein PG, Xia H, Tsien RW (2003) Signaling from synapse to nucleus: the logic behind the mechanisms. Curr Opin Neurobiol 13:354–365
25. Foncea R, Andersson M, Ketterman A, Blakesley V, Sapag-Hagar M, Sugden PH, LeRoith D, Lavandero S (1997) Insulin-like growth factor-I rapidly activates multiple signal transduction pathways in cultured rat cardiac myocytes. J Biol Chem 272: 19115–19124
26. Ibarra C, Estrada M, Carrasco L, Chiong M, Liberona JL, Cardenas C, Diaz-Araya G, Jaimovich E, Lavandero S (2004) Insulin-like growth factor-1 induces an inositol 1,4,5-trisphosphate-dependent increase in nuclear and cytosolic calcium in cultured rat cardiac myocytes. J Biol Chem 279:7554–7565
27. Morales MP, Galvez A, Eltit JM, Ocaranza P, Diaz-Araya G, Lavandero S (2000) IGF-1 regulates apoptosis of cardiac myocyte induced by osmotic-stress. Biochem Biophys Res Commun 270:1029–1035
28. Hetz C, Bono MR, Barros LF, Lagos R (2002) Microcin E492, a channel-forming bacteriocin from *Klebsiella pneumoniae*, induces apoptosis in some human cell lines. Proc Natl Acad Sci USA 99:2696–2701
29. Villena J, Henriquez M, Torres V, Moraga F, Diaz-Elizondo J, Arredondo C, Chiong M, Olea-Azar C, Stutzin A, Lavandero S, Quest AF (2008) Ceramide-induced formation of ROS and ATP depletion trigger necrosis in lymphoid cells. Free Radic Biol Med 44:1146–1160
30. Klemm DJ, Watson PA, Frid MG, Dempsey EC, Schaack J, Colton LA, Nesterova A, Stenmark KR, Reusch JE (2001) cAMP response element-binding protein content is a molecular determinant of smooth muscle cell proliferation and migration. J Biol Chem 276:46132–46141
31. Duchen MR (1999) Contributions of mitochondria to animal physiology: from homeostatic sensor to calcium signalling and cell death. J Physiol 516:1–17
32. Benard G, Bellance N, James D, Parrone P, Fernandez H, Letellier T, Rossignol R (2007) Mitochondrial bioenergetics and structural network organization. J Cell Sci 120:838–848
33. Gunter TE, Buntinas L, Sparagna G, Eliseev R, Gunter K (2000) Mitochondrial calcium transport: mechanisms and functions. Cell Calcium 28:285–296
34. Juretic N, Urzua U, Munroe DJ, Jaimovich E, Riveros N (2007) Differential gene expression in skeletal muscle cells after membrane depolarization. J Cell Physiol 210:819–830
35. Beekman RE, van Hardeveld C, Simonides WS (1988) Effect of thyroid state on cytosolic free calcium in resting and electrically stimulated cardiac myocytes. Biochim Biophys Acta 969:18–27
36. Hallaq H, Hasin Y, Fixler R, Eilam Y (1989) Effect of ouabain on the concentration of free cytosolic Ca^{2+} and on contractility in cultured rat cardiac myocytes. J Pharmacol Exp Ther 248:716–721
37. Erickson GR, Alexopoulos LG, Guilak F (2001) Hyper-osmotic stress induces volume change and calcium transients in chondrocytes by transmembrane, phospholipid, and G-protein pathways. J Biomech 34:1527–1535
38. Fernandes J, Lorenzo IM, Andrade YN, Garcia-Elias A, Serra SA, Fernandez-Fernandez JM, Valverde MA (2008) IP3 sensitizes TRPV4 channel to the mechano- and osmotransducing messenger 5′-6′-epoxyeicosatrienoic acid. J Cell Biol 181:143–155
39. Berridge MJ, Lipp P, Bootman MD (2000) The versatility and universality of calcium signalling. Nat Rev Mol Cell Biol 1:11–21
40. Berridge MJ, Bootman MD, Roderick HL (2003) Calcium signalling: dynamics, homeostasis and remodelling. Nat Rev Mol Cell Biol 4:517–529
41. Wang SQ, Song LS, Lakatta EG, Cheng H (2001) Ca^{2+} signalling between single L-type Ca^{2+} channels and ryanodine receptors in heart cells. Nature 410:592–596
42. Boitano S, Dirksen ER, Sanderson MJ (1992) Intercellular propagation of calcium waves mediated by inositol trisphosphate. Science 258:292–295
43. Rizzuto R, Pozzan T (2006) Microdomains of intracellular Ca^{2+}: molecular determinants and functional consequences. Physiol Rev 86:369–408
44. Carafoli E (2002) Calcium signaling: a tale for all seasons. Proc Natl Acad Sci USA 99:1115–1122
45. Rizzuto R, Brini M, Murgia M, Pozzan T (1993) Microdomains with high Ca^{2+} close to IP3-sensitive channels that are sensed by neighboring mitochondria. Science 262:744–747
46. Orrenius S, Zhivotovsky B, Nicotera P (2003) Regulation of cell death: the calcium-apoptosis link. Nat Rev Mol Cell Biol 4:552–565
47. Gustafsson AB, Gottlieb RA (2008) Heart mitochondria: gates of life and death. Cardiovasc Res 77:334–343
48. Javadov S, Karmazyn M (2007) Mitochondrial permeability transition pore opening as an endpoint to initiate cell death and as a putative target for cardioprotection. Cell Physiol Biochem 20:1–22
49. Criollo A, Galluzzi L, Chiara MM, Tasdemir E, Lavandero S, Kroemer G (2007) Mitochondrial control of cell death induced by hyperosmotic stress. Apoptosis 12:3–18
50. Colell A, Ricci JE, Tait S, Milasta S, Maurer U, Bouchier-Hayes L, Fitzgerald P, Guio-Carrion A, Waterhouse NJ, Li CW, Mari B, Barbry P, Newmeyer DD, Beere HM, Green DR (2007) GAPDH and autophagy preserve survival after apoptotic cytochrome c release in the absence of caspase activation. Cell 129:983–997
51. Holler N, Zaru R, Micheau O, Thome M, Attinger A, Valitutti S, Bodmer JL, Schneider P, Seed B, Tschopp J (2000) Fas triggers an alternative, caspase-8-independent cell death pathway using the kinase RIP as effector molecule. Nat Immunol 1:489–495
52. Scheller C, Knoferle J, Ullrich A, Prottengeier J, Racek T, Sopper S, Jassoy C, Rethwilm A, Koutsilieri E (2006) Caspase inhibition in apoptotic T cells triggers necrotic cell death depending on the cell type and the proapoptotic stimulus. J Cell Biochem 97:1350–1361
53. Chen TY, Chi KH, Wang JS, Chien CL, Lin WW (2009) Reactive oxygen species are involved in FasL-induced caspase-independent cell death and inflammatory responses. Free Radic Biol Med 46:643–655
54. Green DR, Kroemer G (2004) The pathophysiology of mitochondrial cell death. Science 305:626–629
55. Christensen MLM, Braunstein TH, Treiman M (2008) Fluorescence assay for mitochondrial permeability transition in cardiomyocytes cultured in a microtiter plate. Anal Biochem 378:25–31
56. Hwang YC, Kaneko M, Bakr S, Liao H, Lu Y, Lewis ER, Yan S, Ii S, Itakura M, Rui L, Skopicki H, Homma S, Schmidt AM, Oates PJ, Szabolcs M, Ramasamy R (2004) Central role for aldose reductase pathway in myocardial ischemic injury. FASEB J 18:1192–1199
57. Srivastava SK, Ramana KV, Bhatnagar A (2005) Role of aldose reductase and oxidative damage in diabetes and the consequent potential for therapeutic options. Endocr Rev 26:380–392

58. Dragunow M (2004) CREB and neurodegeneration. Front Biosci 9:100–103
59. Shankar DB, Cheng JC, Sakamoto KM (2005) Role of cyclic AMP response element binding protein in human leukemias. Cancer 104:1819–1824
60. Walton M, Woodgate AM, Muravlev A, Xu R, During MJ, Dragunow M (1999) CREB phosphorylation promotes nerve cell survival. J Neurochem 73:1836–1842
61. Pugazhenthi S, Nesterova A, Sable C, Heidenreich KA, Boxer LM, Heasley LE, Reusch JE (2000) Akt/protein kinase B up-regulates Bcl-2 expression through cAMP-response element-binding protein. J Biol Chem 275:10761–10766
62. Wang JM, Chao JR, Chen W, Kuo ML, Yen JJ, Yang-Yen HF (1999) The antiapoptotic gene mcl-1 is up-regulated by the phosphatidylinositol 3-kinase/Akt signaling pathway through a transcription factor complex containing CREB. Mol Cell Biol 19:6195–6206
63. Maldonado C, Cea P, Adasme T, Collao A, Diaz-Araya G, Chiong M, Lavandero S (2005) IGF-1 protects cardiac myocytes from hyperosmotic stress-induced apoptosis via CREB. Biochem Biophys Res Commun 336:1112–1118
64. Kornhauser JM, Cowan CW, Shaywitz AJ, Dolmetsch RE, Griffith EC, Hu LS, Haddad C, Xia Z, Greenberg ME (2002) CREB transcriptional activity in neurons is regulated by multiple, calcium-specific phosphorylation events. Neuron 34:221–233
65. Mayr B, Montminy M (2001) Transcriptional regulation by the phosphorylation-dependent factor CREB. Nat Rev Mol Cell Biol 2:599–609